DOI: 10.24930/1681-9004-2023-23-2-292-302

Magnetic constraints and susceptible inversions of Balapur Fault at central Kashmir Basin, NW Himalaya

Ayaz Mohmood Dar, Syed Kaiser Bukhari

National Institute of Technology Srinagar, Srinagar 190006, India,
e-mails: ayazmohmood@hotmail.com, skbukhari@nitsri.net

Received 10.11.2022, accepted 13.01.2023

Research subject. Subsurface investigations of the Balapur Fault at central Kashmir Basin, NW Himalaya through ground magnetic surveys and data interpretations. *Materials and methods.* The total magnetic intensity data was obtained using ground magnetic surveys carried out by proton precession magnetometers at 15 m spacing. The magnetic constraints and inversions of the Balapur fault in the central Kashmir basin of NW Himalaya were analyzed. *Results.* The total magnetic intensity was found averaging at 97.7 with 45.8 nT as magnetic minima and 140.9 nT as magnetic maxima. The minima's ranging from 45.8 and 55.8 nT in the gridded profile are inferred at the Balapur fault. Further, the fault-related susceptibility index was recorded from 0.0035 SI to 0.0015 SI, and the observed and predicted response values were found ranging between 67.1 to 87.7 and 67.4 to 86.6 nT respectively. *Conclusion.* The study suggests that the Balapur fault in the central Kashmir has produced high subsurface hydraulic activities and, therefore, evident low magnetic anomalies. The analysis reveals a thick minima region related to the fault and also indicated the presence of associated structures with the main Balapur fault segment.

Keywords: *Total magnetic intensity, Magnetic inversions, Balapur fault, Kashmir basin*

Магнитные ограничения и инверсионная восприимчивость разлома Балапур Центрального Кашмира СЗ Гималаев

А. М. Дар, С. К. Бухари

Сринагарский Национальный Технологический институт, г. Сринагар, 190006, Индия,
e-mails: ayazmohmood@hotmail.com, skbukhari@nitsri.net

Поступила в редакцию 10.11.2022 г., принята к печати 13.01.2023 г.

Объект исследования. Балапурский разлом, расположенный в центральной части Кашмирского бассейна в СЗ Гималаях. *Материалы и методы.* Данные общей магнитной интенсивности региона были получены с помощью наземных магнитных съемок, проведенных протонными прецизионными магнетометрами с интервалом 15 м, проводились также исследования магнитных ограничений и инверсий Балапурского разлома. *Результаты*. Установленная средняя магнитная интенсивность усредняется до 97.7 нТл с минимумом 45.8 и максимумом 140.9 нТл. Минимумы в диапазоне от 45.8 до 55.8 нТл получены в сетчатом профиле Балапурского разлома. Кроме того, индекс чувствительности, связанный с отказом, был зарегистрирован от 0.0035 до 0.0015 SI, а наблюдаемые и прогнозируемые значения отклика находились в диапазоне от 67.1 до 87.7 и от 67.4 до 86.6 нТл соответственно. *Выводы.* Предполагается, что Балапурский разлом в Центральном Кашмире вызвал высокую подповерхностную гидравлическую активность и, следовательно, низкие магнитные аномалии. Выявлена область мощных минимумов, связанных с разломом, а также наличие структур, связанных с основной частью Балапурского разлома.

Ключевые слова: *общая магнитная интенсивность, магнитные инверсии, Балапурский разлом, Кашмирский бассейн*

INTRODUCTION

The geomagnetic surveys and data interpretations have intensely developed our ability to analyze the earth's magnetic measurements (Malin, Barraclough, 1982; Cain et al., 1989; Gonzales et al., 1999; Jackson et al., 2000; Kono, Roberts, 2002; Valet, 2003). These measurements have contributed widely to the

Для цитирования: Дар А.М., Бухари С.К. (2023) Магнитные ограничения и инверсионная восприимчивость разлома Балапур Центрального Кашмира СЗ Гималаев. *Литосфера*, **23**(2), 292-302. (англ.) https://doi.org/10.24930/1681-9004-2023-23-2-292-302

For citation: Dar A.M., Bukhari S.K. (2023) Magnetic constraints and susceptible inversions of Balapur Fault at central Kashmir Basin, NW Himalaya. *Lithosphere (Russia)*, **23**(2), 292-302. (In Eng.) https://doi.org/10.24930/1681-9004-2023-23-2-292-302

identification of subsurface geological structures (Henkel, Guzmin, 1977; Dobrin, Savit, 1988; Telford et al., 1990; Arkani et al., 1994; Pilkington, Keating, 2004; Lanza, Meloni, 2006; Dar, Lasitha, 2015). Further, the advancement in computation performance allows us to three-dimensional modeling of magnetic data, and magnetization distribution can be extended to 3D in the subsurface. The subsurface model for anomalous sources can be utilized as rectangular prisms for comprehensive observations. The 3D magnetic inversions are playing a significant role in subsurface evaluations, and the susceptibility inversions algorithms have been widely used in recent times. Several attempts have been successfully attempted in the recent past to formulate the magnetization inversion to overcome the difficulties associated with unknown magnetization (Lelievre, Oldenburg, 2009; Li et al., 2010; Kowalczyk et al., 2010; Sun, Li, 2011; Ellis et al., 2012; Liu et al., 2013; Pilkington, Beiki, 2013; Martinez, Li, 2015). The estimation of the material parameters and geometry of the magnetic source can be obtained by a geophysical inverse problem which converts the observed magnetic data into a model of subsurface magnetization and also reveals the source of the magnetic signal (Tontini et al., 2006). The forward modeling builds a subsurface model using known geological parameters where magnetic signatures of vertical faults can be assessed (Sharma, 1997). The conventionally difficult strong magnetized bodies can be achieved by iterating the convolutions. Several studies have used 3D Fourier convolutions for modeling to magnetic anomalies (Phillips, 2014; Clifton, 2015, 2018). The Fourier convolution multiplies the transform of a function with the transform of a kernel to obtain convolution functions (Blakely, 1995). The intension of our study is to characterize the source depth by numerical integrations and to obtain slabs at depths. The method of obtaining depths was appropriately formulated by previous studies through proper spectra in which the grids were obtained and plotted (Spector, Grant, 1970; Kivior, 1996; Meixner, Jonston, 2012). The concept of equivalent sources was also found significant in modeling the potential field. Various studies have used the modeling procedures ranging from upward or downward continuation transformations to reduction to pole to obtain the heights and magnetization vector (Emilia, 1973; Silva, 1986; Cordell, 1992; Mendonca, 1994, 1995; Cooper, 2000; Dar, 2015; Dar, Lasitha, 2015; Dar et al., 2017). Further, the resolution measure can be developed without any effect by the calculated model to find more realistic lengths (Pilkington, 2016). The method suggests that the resolution length is equal to the depth of the parameter, and therefore the feature of interest can be modeled. Our study aimed to utilize all these studies to frame the 3D subsurface view based on the magnetization factor and to evaluate the structural features. The Balapur fault in Kashmir valley has been widely discussed due to its adequate nature and allied land deformations (Ahmad, Bhat, 2012; Ahmad et al., 2014; Madden et al., 2011). Based on the paleoseismic evidence, the length of the fault was estimated to be ≈40 km in the initial studies. However, recent studies suggest that the fault propagates beyond the estimated length is estimated to at ≈95 km (Ayaz, Bukhari, 2020). The erosional and depositional soft sediment processes have caused certain uncertainties in assessing the actual fault characteristics. Keeping this in view, the present study utilized the magnetic signatures and inversion modeling to evaluate characteristics of the Balapur fault at central Kashmir Basin, NW Himalaya.

GEOLOGY AND TECTONIC SETTING

The Kashmir basin is one of the intermontane basins that lies in the Himalaya region. The Kashmir basin is an oval-shaped basin that is surrounded by mountain ranges from all sides. The basin is surrounded by thrust faulting from all sides (Fig. 1). These thrust zones we formed due to the collision of the Indian and Eurasian plates. The major thrusts include Main Boundary Thrust (MBT), Main Central Thrust (MCT) also known as Panjal Thrust, and Main Mantle Thrust (MMT). The Balapur fault is the longest linear fault in the Kashmir basin whose length is estimated approximately 100 km (Dar, Bukhari, 2020). This fault has been studied widely due to its evident presence and tectonic impressions.

The Kashmir basin consists of a wide range of lithology ranging from agglomerate slates to quaternary deposition. However, the basin is dominantly consisting of quaternary deposits, limestone, and panjal volcanics. The quaternary deposits which are dominant in the basin and have occupied the low-lying base consist of clay, sand, gravel, and clastic material. These deposits have occupied the central region of the Kashmir basin and also make it hard to analyze the geomorphic features of the tectonic setting. Further, the two more dominant lithologies are limestone and panjal volcanics which lie adjacent to the quaternary formation of the Kashmir basin. The other lithologies which are of lesser distribution include Granite, agglomeratic slates, fenestella shale, muree rocks, muth quartzite, and salkhala rocks.

DATA AND METHODS

The ground magnetic surveys at 15 m spacing within 2 km^2 grid were carried out at the Balapur fault located in the central Kashmir basin of NW, Himalaya (Fig. 2). The magnetic surveys were aimed to evaluate the characteristics of subsurface magnetic susceptibilities, structure constraints and inversion modeling at Balapur fault and associated structures. Considering the motive behind the objective, the survey was kept precise for detailed subsurface observations based on magnetization factor. The spacing between the mainframe of the magnetometer and sensor was kept at least >1 m to avoid the magnetic influence of

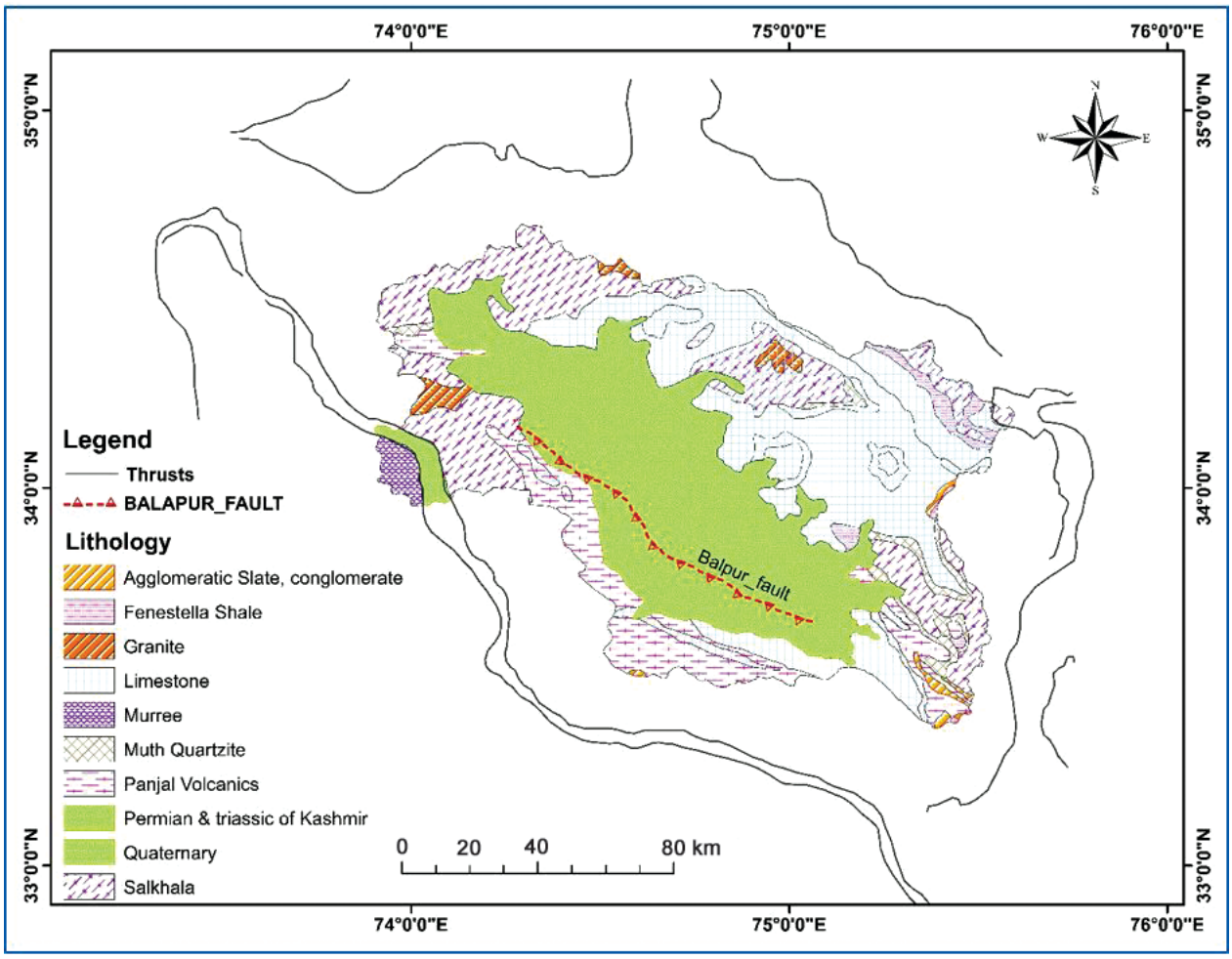

Fig. 1. Geology and Tectonic setting of the Kashmir basin.

Рис. 1. Геология и тектонические особенности Кашмирского бассейна.

the mainframe on the sensor. The magnetic materials carried by the field engineers was kept at least >10 m distant at the time of obtaining earth's magnetic field and >100 m distant from the instrument in case of any metallic infrastructure like electric poles and wires to avoid metallic noises in the field itself. The ground magnetic surveys were carried out in linear profiles to form a grid with approximately 15 m spacing between the two magnetic stations. The earth's magnetic field measurements were recorded thrice at every location to obtain the average value for precise calculations.

Base station data

The base station was used to measure the earth's magnetic field at a certain location frequently to analyze the diurnal magnetic variations. The diurnal variations are the variations of the earth's magnetic field with time and last for several hours to one day. The variations show the timely behavior of the earth's magnetic field element and are interpreted as the superimposition of waves and the influence of magnetic sources that are external to earth. The susceptibilities in the geomagnetic field are also caused by equatorial electro-jet which can lead to a variation of 30 to 200 nT. Further, the calculation of diurnal variation was significant for analyzing the actual total magnetic intensities at field stations by matching the intensities of the base station and field station at the identical time. The base station was situated at places with no or minimum presence of magnetic noise. The data was collected every 30 seconds for precise measurements of diurnal variations and to calculate total magnetic intensities of field data.

Calculation of Total Magnetic Intensities

The total magnetic intensity (TMI) is the reflection of total magnetic susceptibility by geological features based on the magnetization factor. Our study aimed to create the TMI database of surveyed stations to assess the magnetic anomalies at subsurface. The database

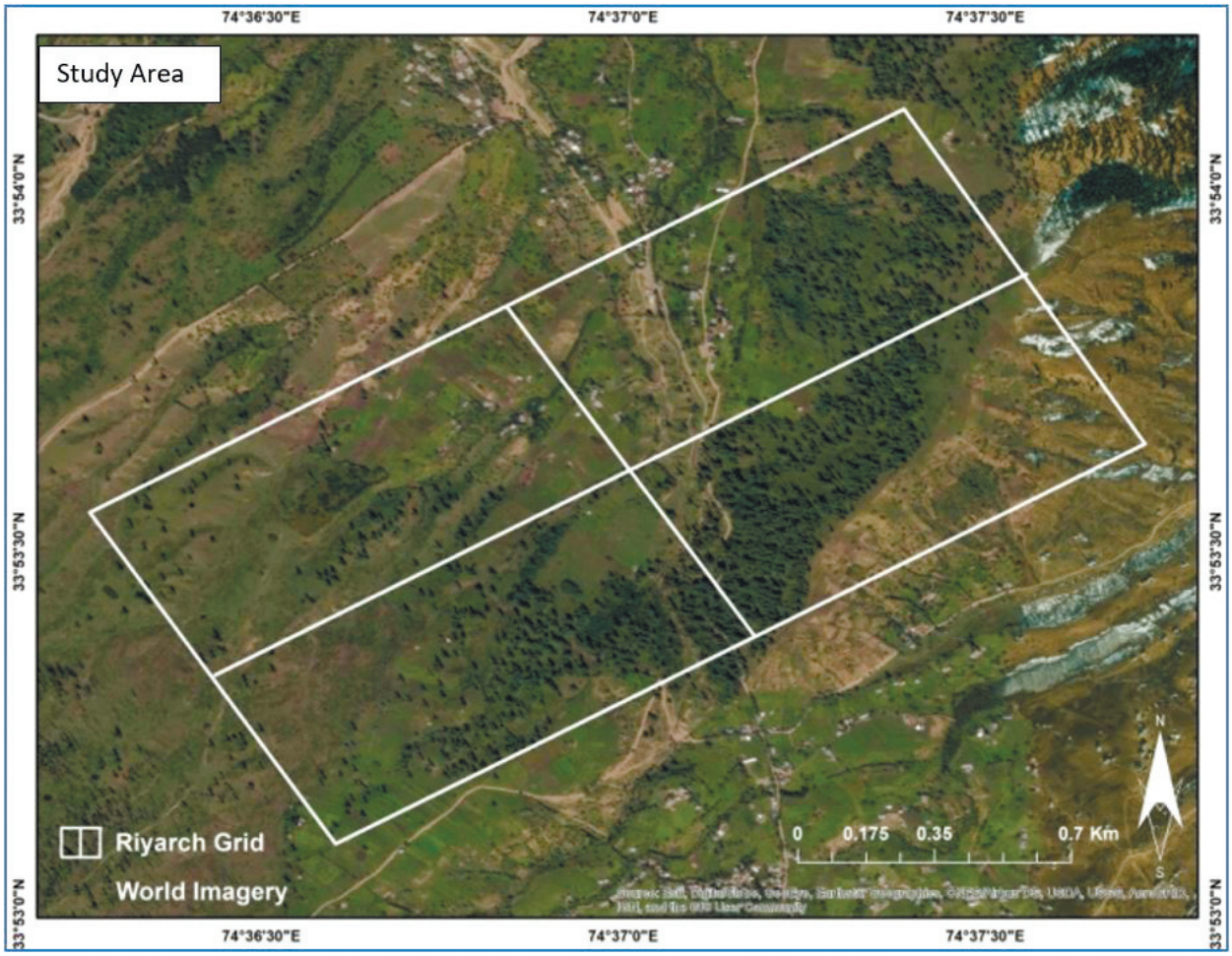

Fig. 2. Study area.

Рис. 2. Площадь исследований.

was created by removing the model of the earth's normal magnetic field and diurnal variations to assess the detailed magnetic characteristics of subsurface faults and related susceptibilities (Eq. 1 and 2):

$$\text{TMI} = f_i - \text{IGRF}, \quad (1)$$

$$f_i = Ip - Dv. \quad (2)$$

Where, is the earth's magnetic field intensity, IGRF is the Magnetic reference model, *Ip* is the average magnetic intensity at a certain point, and *Dv* is the diurnal variation for a particular station.

The average magnetic field intensity at a point (*Ip)* and diurnal variations (*Dv*) were calculated as (Eq. 3 and 4).

$$IP = mi_1 + mi_2 + mi_3/3, \quad (3)$$

$$Dv = m_b - m_i. \quad (4)$$

Where, mi_1, mi_2, and mi_3 represent the normal earth's field magnetic intensities at a certain point, m_b is the earth's magnetic intensity at a base station for a particular time, and I_i is the initial magnetic intensity recorded at the base station.

Inversion modeling

The inversion is the mathematical calculation of data to provide constraints of subsurface susceptibility distribution. The inversion of magnetic data is significant for understanding the subsurface features based on the magnetization of materials. Our study aimed to perform the inversion with susceptibility and their logarithms observe positivity constraint and logarithmic assumptions by iterating small vectors. The parametric inversion was carried out using parameters of a few geometric bodies to obtain the values by nonlinear inversion. Further, the approach of inverting magnetic data was done by dividing the region into smaller cells of unknown susceptibility to recognize the non-uniqueness of the solution. The first step in the inversion approach was to decide the variable for interpretation and to form a multi-component objective function to generate the specific type of model. The interpretations like data checking and editing, magnetic variations, micro leveling, and

data merging and enhancements were carried out before every inversion. The data merging and data enhancements were performed using Geosoft oasis montaj; geophysical software and every database were exported for modeling.

Forward modeling

Forward modeling is the problem of getting the model to produce the data for inputs based on certain parameters. The anomaly at various depths is achieved by numerical integration to provide an inverse model of the number of elemental dipoles. The magnetically varying slabs were obtained at depths by accumulating dipole anomaly at each location. The dipoles of various slabs were also analyzed using power spectra methods and 2D Fourier transformations to evaluate the appearance of various subsurface magnetization distributions. Maxwell's equation was used for 2D-3D forward modeling for static fields with no source and is expressed as (Eq. 5):

$$\nabla.B = 0, \nabla.H = 0. \quad (5)$$

Where (B) is the magnetic flux density and (H) is the magnetic field strength.

The (H) is expressed as the gradient of scalar potential and (B) as constructive relation (Eq. 6 and 7)

$$H = \nabla\varnothing. \quad (6)$$

$$B = \mu H. \quad (7)$$

Where ($\varnothing$) is the gradient and (μ) is the magnetic permeability.

The forward modeling method was used to form the foundation for inversion algorithm with self-demagnetization and discretization.

RESULTS AND DISCUSSION

The Balapur fault was found associated to the magnetic lows ranging from 45.8 and 55.8 nT and the susceptibility index (SI) of –0.0040 to –0.0002 were found associated with the fault. Our study implies that the Balapur fault has produced well developed magnetic constraints throughout its strike. The little or no variation was found between the observed and predicted databases and the analysis recorded the accuracy factor of 0.002 with 20 iterations.

Total magnetic intensity anomalies

The total magnetic intensity was found averaging at 97.7 with 45.8 nT as magnetic minima and 140.9 nT as magnetic maxima. The minima's ranging from 45.8 and 55.8 nT in the gridded survey is associated to the Balapur fault whereas the maxima's ranged from 110 to 140.9 nT was recorded as anomalies related to the hard rock lithology present in the region (Fig. 3). The 52.7 degrees of magnetic inclination and 2.6 degrees magnetic declination of was recorded during analysis.

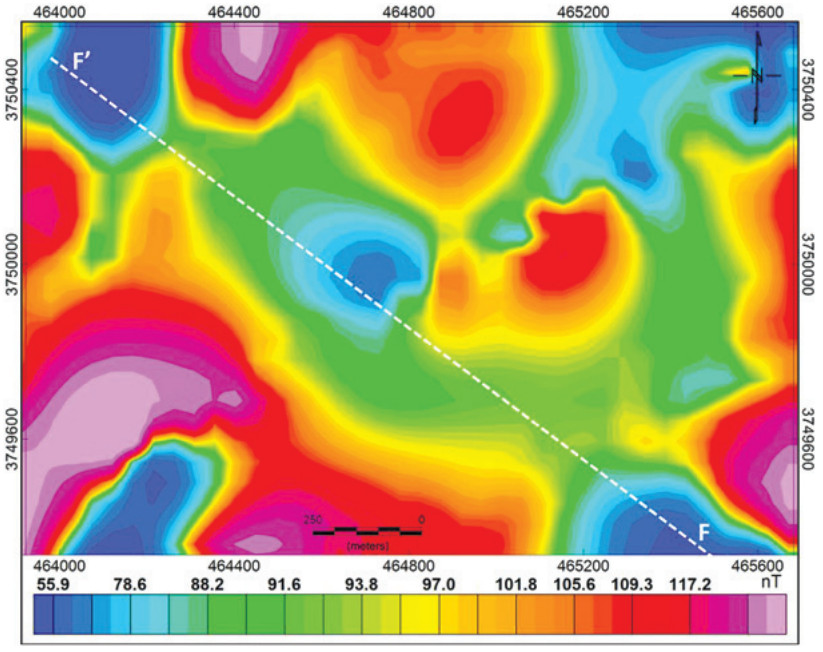

Fig. 3. The map represents the discrepancy and fluctuations of TMI data.

The line F-F' represents the Balapur fault.

Рис. 3. Карта, представляющая несогласия и флуктуации общей магнитной интенсивности (TMI).

Линия F–F' соответствует Балапурскому разлому.

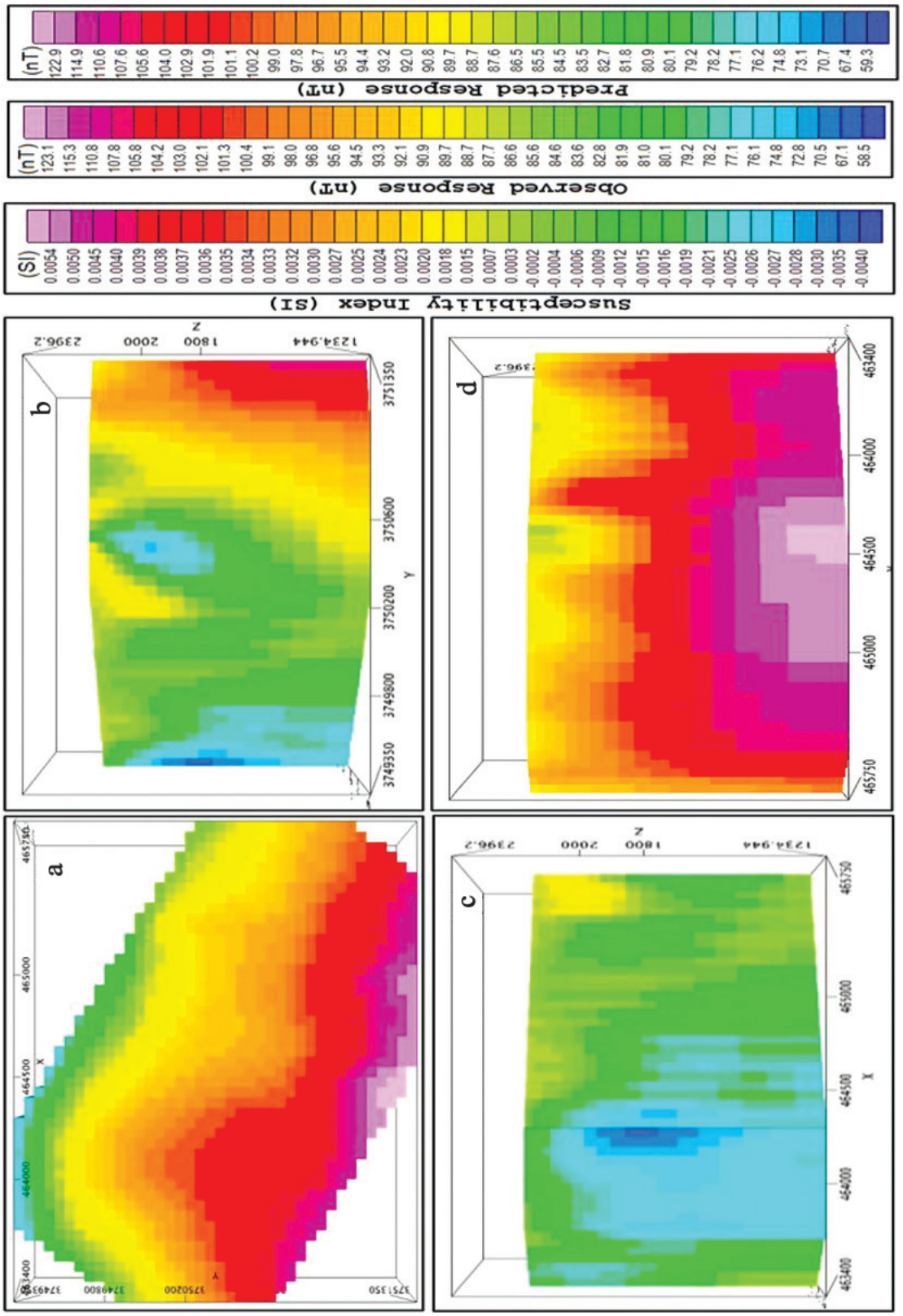

Fig. 4. The map represents the three-dimensional susceptibility index by inversion at Riyar Budgam with matching color legends of observed and predicted responses.
a – top view, b – east view, c – north view, d – south view.

Рис. 4. Индекс трехмерной (магнитной) восприимчивости путем инверсии в Рияр-Буджаме с соответствующими цветовыми обозначениями наблюдаемых и прогнозируемых откликов.
a – вид сверху, b – вид на восток, c – вид на север, d – вид на юг.

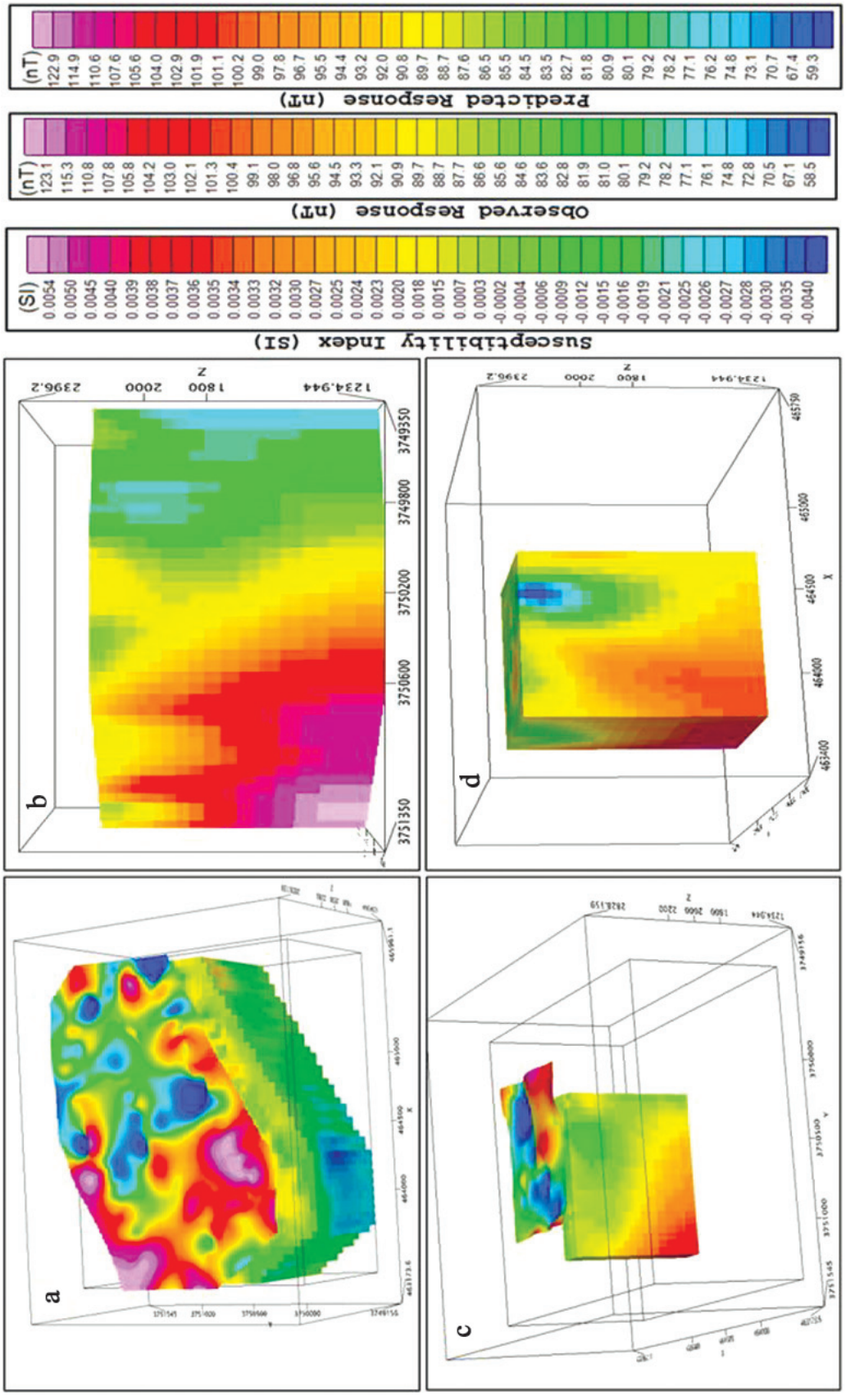

Fig. 5. The map represents the cross sections of material susceptibility at Tangmarg and adjoining areas with matching color legends of observed and predicted responses.

a – sub-surface material susceptibility slab overlain by predicted map, b – sub-surface material susceptibility slab east view, c – material susceptibility slap beneath Balapur fault at central region overlain by predicted map, d – material susceptibility slap in vertical view.

Рис. 5. Поперечные сечения восприимчивого материала в Тангмарге и прилегающих районах с соответствующими цветовыми обозначениями наблюдаемых и прогнозируемых откликов.

а – субповерхностная плита, наложенная на прогнозную карту, b – плита восприимчивого материала недр к востоку, c – плита под Балагурским разломом в центре региона, перекрытого предыдущей картой к востоку, d – восприимчивый материал в вертикальном разрезе.

The anomaly of the lowest range at the central region of the grid depicts the peak influence on the main magnetic field, which can only be caused by the hydraulic activities through the fracture zone.

Data inversions and modeling

The inversion results suggest that the Balapur fault approximately originating at south Kashmir has clear evidence about its presence in the central Kashmir at the foothills of Pir-Panjal mountain range. The fault has produced enough strain and its subsurface magnetization reflections are visible. The observed data were found averaging at 84.95 nT with a standard deviation of 13.59 nT. The predicted response was recorded averaging at 90 nT with the standard deviation of 19.5 nT. The susceptibility transitions are visible in three-dimensional inversion displays (Fig. 4).

The Balapur fault-related susceptibility index was estimated from –0.0035 to 0.0015 SI and the observed and predicted response values were found ranging between 67.1 to 87.7 nT and 67.4 to 86.6 nT respectively. The higher susceptibility index ranging from 0.0034 to 0.0054 as ore deposit channels associated with Balapur fault. The ore channels are found as linear or curvilinear and are mostly associated with the left of the Balapur fault in the North West direction. The observed and predicted response values of the higher magnetic characteristic channels were found ranging from 102 to 123 nT and 101 to 122 nT respectively. Various other curvilinear magnetic transitions zones based on magnetization factors were also recorded and are considered as the difference in the nuclear magnetic strains, however higher than fault zones. Further, the susceptibility slabs in 3D are also portraying the presence of linear low magnetic zones, therefore fault-related anomalies (Fig. 5).

The analysis reveals a thick minima region related to the fault and also indicated the presence of associated structures with the main Balapur fault segment. The inversion of certain rectangular prisms is enormously attributed to the Balapur fault (Fig. 6).

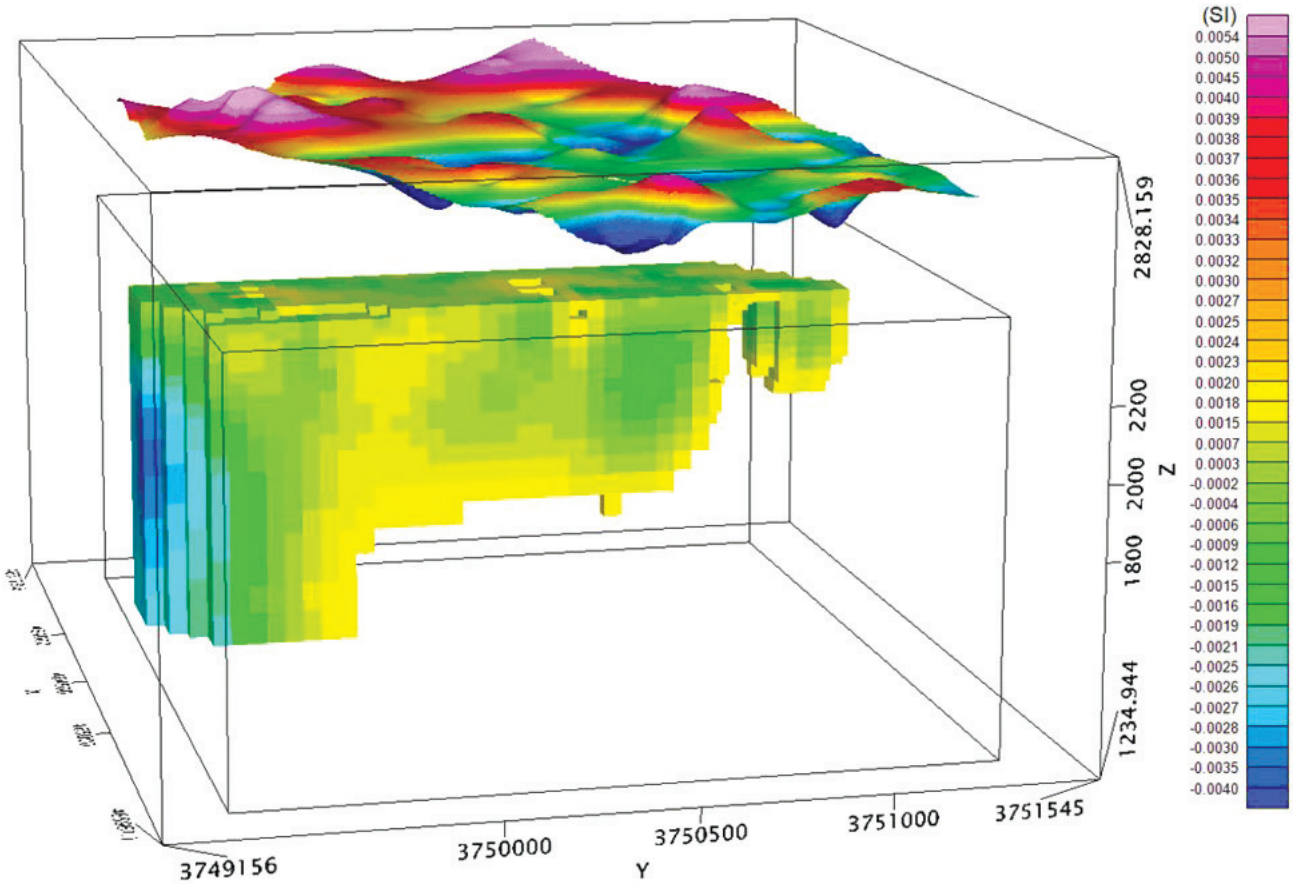

Fig. 6. The map represents the Susceptibility index rectangular prisms of Balapur fault at central Kashmir with matching color legends of observed and predicted responses.

Рис. 6. Прямоугольные призмы индекса восприимчивости разлома Балапур с соответствующими цветовыми обозначениями наблюдаемых и прогнозируемых откликов.

From the prismatic view of rectangular slabs, the fault seems more active. Based on the prismatic view, the fault is seemingly moving forward and therefore needed more assessments. The magnetic cones and the linear and parallel sequence indicate the presence of two fault-related minimal zones (Fig. 7). The total magnetic intensities of the magnetic cones were found ranging between 54 to 60 nT and were recorded as the least intensity magnetization materials. However, few randomly associated magnetic cones portray that the region surrounding Balapur fault may have produced other microstructures too. The results were based on predicated response inversion data and its closeness of database with the observed database signifies the magnetic constraints related to the Balapur fault in central Kashmir. The difference between observed and predicted response databases can be seen in Fig. 8.

CONCLUSIONS

The Kashmir valley has witnessed devastating earthquakes in the past and can occur in the future too. The seismic gap produced by the large magnitude earthquakes in the basin has made people reluctant to consider the seismic guidelines for the infrastructural setup. Further, the gap between the seismologists and engineers has amplified the developmental policies related to the risk-based design decisions in the Kashmir

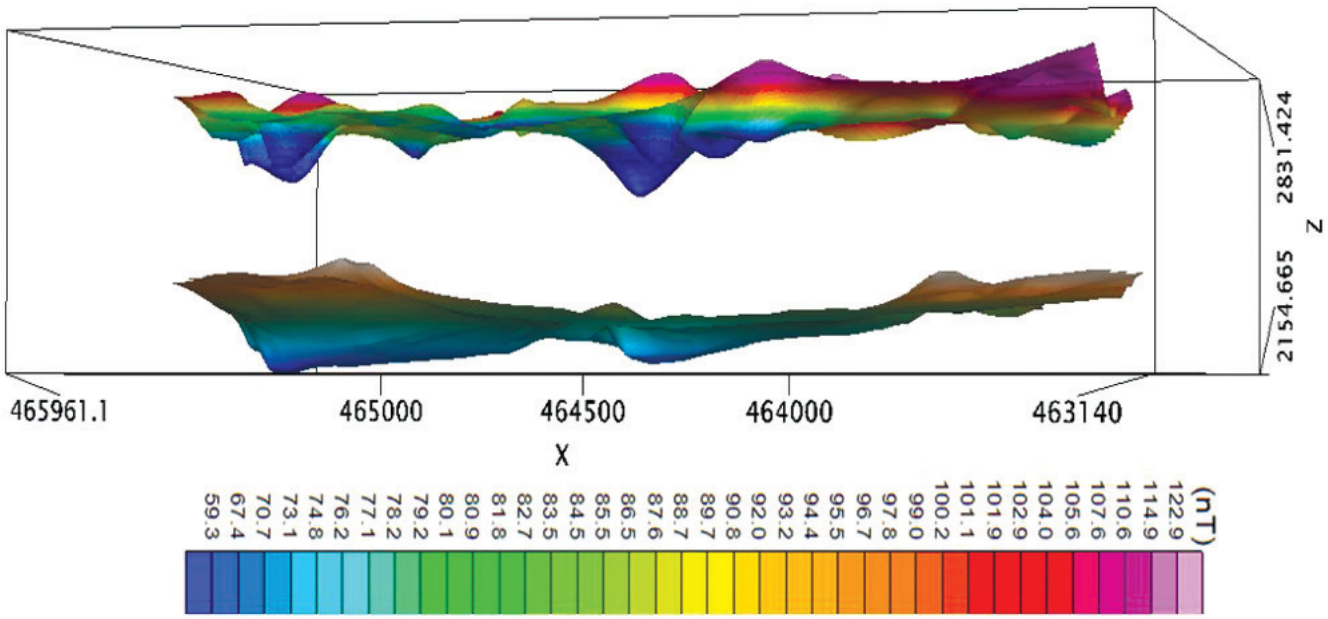

Fig. 7. The map represents the predicted Susceptibility grid and topographic view of Riyar gridded magnetic data.

Рис. 7. Карта прогнозируемой сетки восприимчивости и топографический вид магнитных данных Riyar с привязкой к сетке.

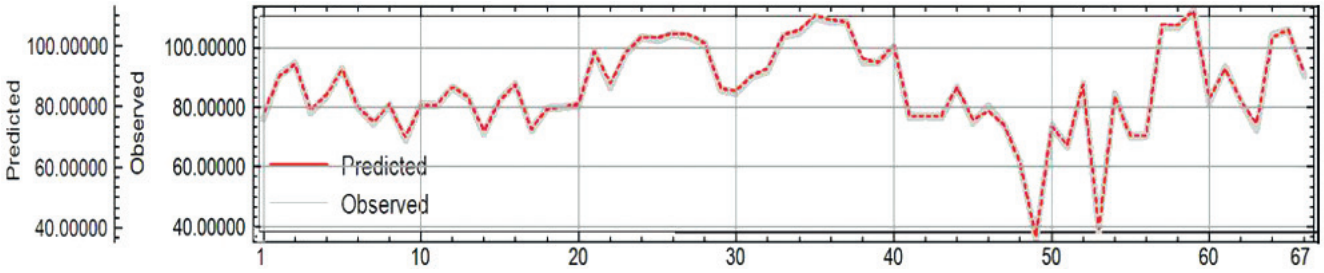

Fig. 8. The map represents the ($d^{obs} - d^{pred}$) for inversion test and a comparison of the profiles.

The observed data profile is grey with the predicted data profile overlaid in red.

Рис. 8. Карта, представляющая ($d^{obs} - d^{pred}$) для проверки инверсии и сравнения профилей.

Наблюдаемый профиль данных выделен серым, а прогнозируемый перекрывается красным.

valley. The magnetic data and inversion models suggest that the observed total magnetic intensity anomalies related to the Balapur fault are accurate with the accuracy factor of 0.002 and produce visible subsurface magnetization constraints. The study suggests that the faults are directly associated with magnetic minima's and are due to the oxidation by invading hydraulic fluids at fracture zones. The inversion results show the clear evidence of Balapur fault at the central Kashmir. The fault has produced enough strain and its subsurface magnetization reflections are visible. The observed data were found averaging at 84.95 nT with a standard deviation of 13.59 nT. The predicted response was recorded averaging at 90 nT with the standard deviation of 19.5 nT. The fault mapping and investigations of fault characteristics using ground magnetic methods was found significant by appropriate field surveys and convenient interpretations and hence can be used for subsurface fault characterization.

REFERENCES

Ahmad S., Bhat M.I. (2012) Tectonic geomorphology of the Rambiara basin, SW Kashmir Valley reveals emergent out-of-sequence active fault system. *Himal. Geol.*, **33**(2), 162-172.

Ahmad S., Bhat M.I., Madden C., Bali B.S. (2014) Geomorphic analysis reveals active tectonic deformation on the eastern flank of the Pir-Panjal range, Kashmir Valley, India. *Arab. J. Geosci.*, **7**(2225-2235). https://doi.org/10.1007/s12517-013-0900-y

Arkani-Hamed J., Langel R.A., Purucker M. (1994) Magnetic anomaly maps of the Earth derived from POGO and Magsat data. *J. Geophys. Res.*, 99:24075-24090.

Blakely R.J. (1995) Potential theory in gravity and magnetic applications. Cambridge University Press, Cambridge, UK.

Cain J.C., Wang Z., Schmitz D.R., Meyer J. (1989) The geomagnetic spectrum for 1980 and core crustal separation. *Geophys. J.*, 97: 443-447.

Clifton R. (2015) Magnetic depths to basalts: extension of spectral depths method. *Explor. Geophys.*, **46**(3), 284-296. https://doi.org/10.1071/EG13096

Clifton R. (2018) Magnetic depth transects of the Northern Territory. Northern Territory Geological Survey, Digital Information Package DIP 020.

Cooper G.R.J. (2000) Gridding Gravity Data Using an Equivalent Layer. *Comput. Geosci.*, **26**(2), 227-233. https://doi.org/10.1016/S0098-3004(99)00089-8

Cordell L. (1992) A Scattered Equivalent-Source Method for Interpolation and Gridding of Potential-Field Data in Three Dimensions. *Geophysics*, **57**(4), 629-636. https://doi.org/10.1190/1.1443275

Dar A.M. (2015) An Approach of Remote Sensing and GIS for the Delineation of Lineaments in the Suru Valley (Ladakh Himalayas). *J. Remote Sensing GIS*, **4**(2), 4:144, https://doi.org/10.4172/2469-4134.1000144

Dar A.M., Bukhari S.K. (2020) Characteristics of magnetic anomalies and subsurface structure constraints of Balapur fault in Kashmir basin, NW Himalaya. *Phys.Earth Planet. Inter.*, **309**, 106599. https://doi.org/10.1016/j.pepi.2020.106599

Dar A.M., Lasitha S. (2015) Application of Geophysical Ground Magnetic Method for the Delineation of Geological Structures: A Study in Parts of Villupuram District, Tamilnadu. *J. Geol. Geophys.*, **4**(3), 4:209. https://doi.org/10.4172/jgg.1000209

Dar A.M., Lasitha S., Bukhari K., Yousuf M. (2017) Delineating Deep Basement Faults in Eastern Dharwar Craton through Systematic Methods of Geophysics and Remote Sensing vis-à-vis the Concerns of Moderate Seismicity. *J. Geogr. Nat. Disast.*, **7**(1), 7:184. https://doi.org/10.4172/2167-0587.1000184

Dobrin M.B., Savit C.H. (1988) Introduction to Geophysical Prospecting. 4th Edition. McGraw-Hill, N. Y., 867 p.

Ellis R., de Wet B., Macleod I.M. (2012) Inversion of magnetic data from remanent and induced sources. *Presented at the 22nd ASEG International Geophysical Conference*. Australia Society of Exploration Geophysicists.

Emilia D.A. (1973) Equivalent Sources Used as an Analytic Base for Processing Total Magnetic Field Profiles. *Geophysics*, **38**(2), 339-348. https://doi.org/10.1190/1.1440344

Gonzales W.D., Tsuritani B., Clua De Gonzales A. (1999) Interplanetary origin of geomagnetic storms. *Space Sci. Rev.*, **88**, 529-562. http://solid_earth.ou.edu/ notes/ potential/legendre.gif (Copyright 2004, J. Ahern)

Grauch V.J.S., Hudson M.R., Manor S.A. (2000) Aeromagnetic signatures of intrabasinal faults, Albuquerque basin, New Mexico: Implications for layer thickness and magnetization: SEG Technical Program Expanded Abstracts, 363-366.

Henkel H., Guzmin M. (1977) Magnetic feature of fracture zones. *Geoexploration*, **15**(3), 173-181.

Jackson A., Jonkers A.R.T., Walker M.R. (2000) Four centuries of geomagnetic secular variation from historical records. *Philos. T. Roy Soc. A.*, **358**(1768), 957-990. https://doi.org/10.1098/rsta.2000.0569

Kivior I. (1996) A geophysical study of the structure and crustal environment of the Polda Rift, South Australia. Ph.D. thesis. Department of Geology and Geophysics. The University of Adelaide.

Kono M., Roberts H.R. (2002) Recent geodynamo simulations and observations of the geomagnetic field. *Rev. Geophys.*, **40**(4), 4-1-4-53, https://doi.org/10.1029/2000RG000102

Kowalczyk P., Oldenburg D., Phillips N., Nguyen T.H., Thomson V. (2010) Acquisition and analysis of the 2007-2009 geoscience bc airborne data: Australian Society of Exploration Geophysicists – PESA Airborne Gravity Workshop.

Lanza R., Meloni A. (2006) The Earth's Magnetism: An Introduction for Geologists. N. Y., Berlin: Springer, 278 p.

Lelievre P.G., Oldenburg D.W. (2009) A 3d total magnetization inversion applicable when significant, complicated remanence is present. *Geophysics*, **74**(3), L21-L30.

Li Y., Shearer S., Haney M., Dannemiller N. (2010) Comprehensive approaches to 3d inversion of magnetic data affected by remanent magnetization. *Geophysics*, **75**(1), L1-L11.

Liu S., Hu X., Liu T., Feng J., Gao W., Qiu L. (2013) Magnetization vector imaging for borehole magnetic data based on magnitude magnetic anomaly. *Geophysics*, **78**(6), D429-D444.

Madden C., Ahmad S., Meigs A. (2011) Geomorphic and paleoseismic evidence for late Quaternary deformation in the southwest Kashmir Valley, India: Out of-sequence thrusting, or deformation above a structural ramp? *Amer. Geophys. Union Abstr.*, T54B-07.

Malin S.R.C., Barraclough D.R. (1982) 150th anniversary of Gauss's first absolute magnetic measurement. *Nature*, **297**, 285.

Martinez C., Li Y. (2015) Lithologic characterization using airborne gravity gradient and aeromagnetic data for mineral exploration: A case study in the Quadrilatero´ Ferr´ıfero, Brazil: Interpretation.

Meixner A.J., Johnston S. (2012) An iterative approach to optimising depth to magnetic source using the spectral method. ASEG 22nd Geophysical Conference and Exhibition, Brisbane 2012.

Mendonca C.A., Silva J.B.C. (1994) The Equivalent Data Concept Applied to the Interpolation of Potential Field Data. *Geophysics*, **59**(5), 722-732. https://doi.org/10.1190/1.1443630

Mendonca C.A., Silva J.B.C. (1995) Interpolation of Potential-Field Data by Equivalent Layer and Minimum Curvature: A Comparative Analysis. *Geophysics*, **60**(2), 399-407. https://doi.org/10.1190/1.1443776

Phillips J.D. (2014) Using vertical Fourier transforms to invert potential-field data to magnetization or density models in the presence of topography. *SEG Technical Program Expanded Abstracts 2014*, 1339-1343. https://doi.org/10.1190/segam2014-0226.1

Pilkington M. (2016) Resolution measures for 3D magnetic inversions. *Geophysics*, **81**(2), J15-J23. https://doi.org/10.1190/GEO2015-0081.1

Pilkington M., Beiki M. (2013) Mitigating remanent magnetization effects in magnetic data using the normalized source strength. *Geophysics*, **78(**3), J25-J32. https://doi.org/10.1190/geo2012-0225.1

Pilkington M., Keating P. (2004) Contact mapping from gridded magnetic data–a comparison of techniques. *Explor. Geophys.*, **35**(4), 306-311. https://doi.org/10.1071/EG04306

Sharma P.V. (1997) Environmental and engineering geophysics. Cambridge University Press. Cambridge, UK.

Silva J.B.C. (1986) Reduction to the Pole as an Inverse Problem and Its Application to Low-Latitude Anomalies. *Geophysics*, **51**(2), 369-382. https://doi.org/10.1190/1.1442096

Spector A., Grant F.S. (1970) Statistical models for interpreting aeromagnetic data. *Geophysics*, **35**(2), 293-302.

Sun J., Li Y. (2011) Geophysical inversion using petrophysical constraints with application to lithology differentiation. 81st SEG Annual Meeting, 2644-2648.

Telford W.M., Geldhart L.P., Sheriff R.E. (1990) Applied Geophysics (second ed.). Cambridge University Press, Cambridge, 770 p.

Tontini F.C., Cocchi L., Carmisciano C. (2006) Depth-to-the-bottom optimization for magnetic data inversion: Magnetic structure of the Latium volcanic region, Italy. *J. Geophys. Res.*, **111**(B11), B11104. https://doi.org/10.1029/2005JB004109

Valet J.P. (2003) Time variations in geomagnetic intensity. *Rev. Geophys.*, **41**(1), 4:1-44. https://doi.org/10.1029/2001RG000104